ISSN 1392 - 1207. MECHANIKA. 2013 Volume 19(2): 150-158

Numerical study on turbulent flow forced-convection heat transfer for air in a channel with waved fins

H. Benzenine*, R. Saim, S. Abboudi***, O. Imine******

**Department of Mechanical Engineering, Faculty of Mechanical Engineering, University of Science and Technology (USTO), BP 1505 El M'naouar Oran, Algeria, E-mail: b.hamidou@yahoo.fr*

***Laboratory of Energetic and Applied Thermal (ETAP), Faculty of Technology, University Abou Bakr Belkaid, BP 230 - 13000-Tlemcen-Algeria, E-mail: saimrachid@yahoo.fr*

****IRTES-M3M, EA 7274, University of Technology of Belfort Montbeliard (UTBM), Sévenans site-90010-Françe, E-mail: Said.Abboudi@utbm.fr*

*****Laboratory of Aeronautics and Propulsive System, Faculty of Mechanical Engineering,University of Science and Technology (USTO), BP 1505 El M'naouar Oran, Algeria, E-mail: Imine_omar@yahoo.fr*

crossref http://dx.doi.org/10.5755/j01.mech.19.2.4154

1. Introduction

There are several situations where turbulent forced convection occuring in many industrial engineering applications require the use of heat exchangers with tubes arrangements, either finned or no finned, functioning as heat exchangers in air conditioning systems, refrigeration, heaters, plat solar collectors, radiators, etc. The performance of a heat exchanger can be improved by enhancing the heat transfer between the heat exchanger fluids. The objective of the heat transfer augmentation can be achieved by increasing the surface heat transfer coefficient through improving the thermal contact of the heat exchanger fluid with the wall (for example see Nasiruddin and Kamran [1]). There are numerous ways to increase the heat transfer which include, treated surfaces, rough surfaces, extended surfaces, coiled tubes, surface vibration, fluid vibration and jet impingement. A few studies have shown that the heat transfer enhancement can also be achieved by creating longitudinal vortices in the flow. These vortices are produced by introducing an obstacle in the flow, known as a vortex generator (for example, see Fiebig et al., [2]; O'Brien et al., [3]).

This class of heat transfer has been the subject of many experimental and numerical studies. Wilfried and Deiying [4] analyzed the influence of baffle/shell leakage flow on the thermal performance in baffled shell-and-tube heat exchangers with different distances between baffles is studied experimentally. With a shell-side dispersive Peclet number, the axial dispersion model is introduced to analyze the experimental results. The degree of dispersion is characterized by the Peclet number, and its dependence on the clearance between baffles and shell and on the distance between baffles is determined. Rajendra et al. [5] conducted an experimental work on the study of heat transfer and friction in rectangular ducts with baffles (solid or perforated) attached to one of the broad walls. The Reynolds number of the study ranges from 2850 to 11500. The baffled wall of the duct is uniformly heated while the remaining three walls are insulated. These boundary conditions correspond closely to those found in solar air heaters. Over the range of the study, the Nusselt number for the solid baffles is higher than that for the smooth duct, while for the perforated baffles. The friction factor for the solid baffles is found to be 9.6–11.1 times of the smooth duct, which decreased significantly for the perforated baffles with the increase in the open area ratio. Performance comparison with the smooth duct at equal pumping power shows that the baffles with the highest open area ratio give the best performance.

Gupta et al. [6] presented an experimental study on the use of a helical-shape baffle in a mineral (Carbosep) membrane provided an increase of more than 50% in permeate flux compared with that obtained without a baffle at the same hydraulic dissipated power. The effect of the number of helices with respect to baffle length shows that the permeate volume increases with increasing number of helices but to a lesser degree when the number of helices is more than 4 per 25-mm baffle length. Also, when the baffle's maximum diameter was reduced a small variation in permeate flux values was observed. Flow visualization was made with a video camera (VHS) and showed that the flow was rotational around the baffle axis and that the rotational velocity increased the mixing and migration of the rejected particles from the membrane surface.

The hydrodynamics and heat transfer characteristics of a heat exchanger with single-helical baffles are studied experimentally as well as numerically by Yong-Gang Lei et al [7]. A heat exchanger with two-layer helical baffles is designed by using computational fluid dynamics (CFD) method. The comparisons of the performance of three heat exchangers with single-segment baffles, single-helical baffles and two-layer helical baffles, respectively, are presented in the paper. The experiment is carried out in counter-current flow pattern with hot oil in shell side and cold water in tube side. It shows that the heat exchangers with helical baffles have higher heat transfer coefficient to the same pressure drop than that of the heat exchanger with segmental baffles based on the present numerical results, and the configuration of the two-layer helical baffles has better integrated performance than that of the single-helical baffles.

Kang-Hoon Ko et al. [8] have conducted an experimental investigation to measure module average heat transfer coefficients in uniformly heated rectangular channel with wall mounted porous baffles. Baffles were mounted alternatively on top and bottom of the walls. Heat transfer coefficients and pressure loss for periodically fully developed flow and heat transfer were obtained for different types of porous medium and with two window cut

ratios and two baffle thickness to channel hydraulic diameter ratios. Reynolds number (*Re*) was varied from 20.000 to 50.000. To compare the effect of foam metal baffle, the data for conventional solid-type baffle were obtained. The experimental procedure was validated by comparing the data for the straight channel with no baffles with those in the literature. The use of porous baffles resulted in heat transfer enhancement as high as 300% compared to heat transfer in straight channel with no baffles. However, the heat transfer enhancement per unit increase in pumping power was less than one for the range of parameters studied in this work. Correlation equations were developed for heat transfer enhancement ratio and heat transfer enhancement per unit increase in pumping power in terms of Reynolds number.

Ahmet Tandiroglu [9] studied the effect of the flow geometry parameters on transient forced convection heat transfer for turbulent flow in a circular tube with baffle inserts has been investigated. The characteristic parameters of the tubes are pitch to tube inlet diameter ratio, baffle orientation angle. Air, Prandtl number of which is 0.71, was used as working fluid, while stainless steel was considered as pipe and baffle material. During the experiments, different geometrical parameters such as the baffle spacing *H* and the baffle orientation angle *b* were varied. Totally, nine types of baffle inserted tube were used. The general empirical equations of time averaged Nusselt number and time averaged pressure drop were derived as a function of Reynolds number corresponding to the baffle geometry parameters of pitch to diameter ratio *H/D*, baffle orientation angle *b*, ratio of smooth to baffled cross-section area and ratio of tube length to baffle spacing were derived for transient flow conditions. The range of Reynolds number $3000 \leq Re \leq 20000$ for the case of constant heat flux.

An experimental study was conducted by Molki and Mostoufizadeh [10] to investigate heat transfer and pressure drop in a rectangular duct with repeated-baffle blockages. The baffles are arranged in a staggered fashion with fixed axial spacing. The transfer coefficients are evaluated in the periodic fully developed and entrance regions of the duct. The presence of the bathes enhances these coefficients. The entrance length of the duct is substantially reduced by the baffles. Pressure drop and heat transfer data are employed to evaluate the thermal performance of the duct.

Rajendra and Maheshwari [11] present results of an experimental study of heat transfer and friction in a rectangular section duct with fully perforated baffles or half perforated baffles at relative roughness pitch affixed to one of the broader walls. The Reynolds number of the study ranges from 2700 to 11150. The baffled wall of the duct is uniformly heated while the remaining three walls are insulated. The study shows an enhancement of 79–169% in Nusselt number over the smooth duct for the fully perforated baffles and 133–274% for the half perforated baffles while the friction factor for the fully perforated baffles is 2.98–8.02 times of that for the smooth duct and is 4.42–17.5 times for the half perforated baffles. In general, the half perforated baffles are thermo-hydraulically better to the fully perforated baffles at the same pitch. Of all the configurations studied, the half perforated baffles at a relative roughness pitch of 7.2 give the greatest performance advantage of 51.6–75% over a smooth duct at equal pumping power.

According to this literature review, we note that little works have been devoted to studies of the effects of the waved fins and/or baffles on the flow of heat transfer in heat exchangers. The objective in this paper is to quantify numerically the heat transfer by forced convection for different velocities of flow and analyze the geometrical and physical effects of the corrugated fins on heat transfer.

2. Numerical modeling

2.1. Equations governing

The physical system studied is shown in Fig. 1. The flow regime is assumed turbulent, two-dimensional (2D) and stationary. The fluid is assumed Newtonian and incompressible. In order to improve heat transfer, two waved baffles were used in the rectangular duct study. The first baffle is attached to the upper wall of the channel and the second to the lower wall, see Fig. 1, a. The shape and dimensions of a corrugated fin are shown in Fig. 1, b.

The followings assumptions were taken into account:

1. the thermo physical characteristics of the fluid are assumed constant;
2. a profiles of velocity and temperature are assumed uniform at the entrance;
3. the temperatures applied to the walls of the duct are considered constants;
4. The transfer of heat by radiation is negligible.

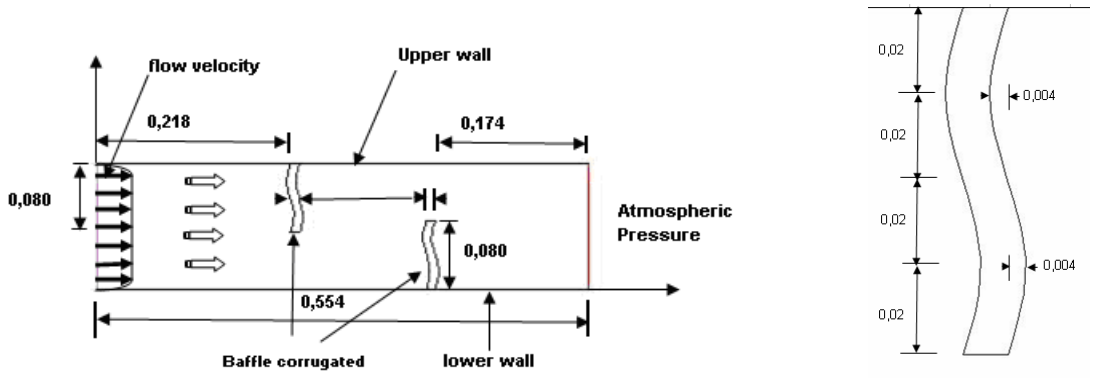

a b

Fig. 1 Schematic configuration of the physical model. (dimensions in m): a) Geometry of the problem under investigation; b) Dimensions of the waved fin

Under these conditions, the equations expressing the conservation of mass, momentum and energy are written as:

$$\nabla \vec{V} = 0; \tag{1}$$

$$\rho\left(\vec{V}\nabla\vec{V}\right) = -\nabla P + \mu_f \Delta\vec{V}; \tag{2}$$

$$\rho C_p\left(\vec{V}\nabla T\right) = \lambda_f \Delta T, \tag{3}$$

where: $\vec{V}$ is the velocity vector; P is the pressure; ρ, μ_f and C_p are respectively the density, the dynamics viscosity and specific heat of fluid.

From a comparative study of four turbulence models, namely the Spalart Allamaras model, the k-ε model, the k-ω model and Reynolds Stress model were evaluated by solving Navier–Stokes equations, it appears that the k-ω model is one who predicts more accurately the changes of flow in the presence of baffles [12]. Another advantage of this model is because it is suitable for both near and distant wall.

The k-ω model is defined by two transport equations, one for the turbulent kinetic energy, k and the other for the specific dissipation rate ε [1], as given below:

$$\frac{\partial}{\partial x_i}\left(\rho\, k\, u_i\right) = \frac{\partial}{\partial x_j}\left(\Gamma_K \frac{\partial k}{\partial x_j}\right) + G_K - Y_K + S_K; \tag{4}$$

$$\frac{\partial}{\partial x_i}\left(\rho\omega\, u_i\right) = \frac{\partial}{\partial x_j}\left(\Gamma_\omega \frac{\partial \omega}{\partial x_j}\right) + G_\omega - Y_\omega + D_\omega + S_\omega \tag{5}$$

or

$$G_K = -\rho\overline{u_i' u_j'}\frac{\delta u_j}{\delta x_i}; \tag{6}$$

$$G_\omega = \alpha\frac{\omega}{k}G_k \tag{7}$$

and

$$\Gamma_k = \mu + \frac{\mu_t}{\sigma_k} \quad \text{and} \quad \Gamma_\omega = \mu + \frac{\mu_t}{\sigma_\omega}, \tag{8}$$

where: Γ_k, Γ_ω are the effective diffusivity of k and ω, x_i, x_j are the spatial coordinates; G_k is the turbulent kinetic energy generation due to mean velocity gradient; G_ω is the kinetic energy generation due to buoyancy; Y_k, Y_ω are the dissipation of k and ω; S_k, S_ω are the source term for k and ω; D_ω is the cross diffusion term; σ_k, σ_ω are the turbulent Prandtl number and α is the coefficient of thermal expansion.

Generally, the main sources of errors in results of the *Nusselt* numbers are statistical uncertainty of surface mean-temperatures and bulk temperature of the fluid. Considering that the computation is confined in one cycle and the difference between wall temperature T_w and bulk (mean) temperature $T_b(x)$:

$$T_{f,m} = T_b(x) = \frac{\int_A u(x,y)T(x,y)dA}{\int_A u(x,y)dA}. \tag{9}$$

The corresponding local and averaged Nusselt numbers are:

$$Nu(x) = \frac{h(x)D_h}{\lambda_f} = \frac{q_w D_h}{\lambda_f\left(T_w - T_b\right)} \tag{10}$$

and

$$\overline{Nu} = \frac{\bar{h}D_h}{\lambda_f}, \tag{11}$$

where: D_h is the hydraulic diameter of the duct; h is heat transfer coefficient and q_w is the heat flux.

The characteristic length is the equivalent diameter of the duct:

$$D_h = 4Hl/2\left(H+l\right), \tag{12}$$

where H and l are the width and length of channel.

The Reynolds number for the rectangular duct is then defined by:

$$R_e = \frac{D_h U\rho}{\mu}. \tag{13}$$

The coefficient of friction and pressure drop in different sections are calculated using the relationship:

$$f = \frac{2\tau_w}{\rho U^2}; \tag{14}$$

$$\Delta P = \frac{fL\rho U^2}{2h}, \tag{15}$$

where τ_w is the wall shear stress.

2.2. Boundary conditions

This work adopts a turbulent flow of air. The hydrodynamic boundary conditions are chosen according to the works of Demartini et al. [13]. The thermal boundary conditions are chosen according to the work of Nasiruddin et al [1]. A uniform velocity is applied at the inlet of the computational domain. The pressure at the inlet of the computational domain was set equal to the zero gauges. A constant temperature of 102°C (375 K) was applied on the entire wall of the computational domain as the thermal boundary condition. The temperature of the working fluid was set equal to 27°C (300 K) at the inlet of the tube. The computational domain and boundaries are presented as:

a) Inlet boundary.

The air is taken at ambient conditions:

$$u = U_{in}, \; v = 0; \tag{16}$$

$$k_{in} = 0.005U_{in}^2; \tag{17}$$

$$\varepsilon_{in} = 0.1\, k_{in}^2; \tag{18}$$

$$T = T_{in}, \tag{19}$$

where: u and v are velocity components in the x and y direction; k_{in} is the inlet condition for the turbulent kinetic energy and ε_{in} is the inlet condition for the dissipation rate.

b) The upper and the lower wall.

The upper and the lower wall of the channel we have:

$$u = v = 0; \tag{20}$$

$$k = \varepsilon = 0; \tag{21}$$

$$T = T_p. \tag{22}$$

c) Exit boundary.

$$P = P_{atm}. \tag{23}$$

d) Fluid solid interface.

The following conditions are applied:

$$\lambda_f \frac{\partial T_f}{\partial n} = \lambda_s \frac{\partial T_s}{\partial n} \quad \text{and} \quad T_f = T_s, \tag{24}$$

where: n is the coordinate normal to the interface; λ_f and λ_s are thermal conductivity of fluid and solid.

3. Numerical solution procedure

For the numerical solution of the system of equations described above, we used the finite volume method. The SIMPLE algorithm developed by Patankar [14] was used for the convective terms in the solution equations. The second order up winding scheme was used to calculate the derivatives of the flow variables. A non-uniform grid is used depending on the cases studied, with a refinery in areas containing baffles and close to walls, to capture the strong gradients of temperature and speed. The method of extending the field is applied [15, 16] for the treatment of solid-fluid interface. A high value is attributed to the viscosity in the equation of momentum to simulate the solid. To ensure independence of the mesh with the results, a series of tests was performed. The iterative solution is continued until the residuals for all cells of calculation are lower than 10^{-8} for all parameters analyzed.

4. Results

4.1. Mesh validation

Different grids were tested for the validity of the mesh and the accuracy of calculations. The results obtained for horizontal and vertical velocities and stream function for a Reynolds number equal at 8.73×10^4, are presented in Table. For the remainder of the study, we chose the grid (124 mm × 33 mm) which provides a precision fit and a relative error between the values found less than 2.3%.

Table

Comparison of results for different mesh grids

Grille	53×10	61×18	94×22	24×33
X, m	0.554	0.554	0.554	0.554
Y, m	0.16	0.16	0.16	0.16
Ψ_{max}, m^2/s	2.054	2.018	2.026	2.048
U_{max}, m^2/s	32.41	34.64	35.70	35.77
V_{max}, m^2/s	28.96	29.97	32.44	31.70

4.2. Model validation

To validate the numerical scheme, we compared our results with those of L. C. Demartini et al. [13]. These authors have studied this problem by numerical and experimental way [13]. Under the same conditions, we present a comparison of velocity profiles at the x = 0.159 m from the entrance of the channel, Fig. 2, and at x = 0.525 m, Fig. 3. These figures show very acceptable agreement between our results and those of the bibliography.

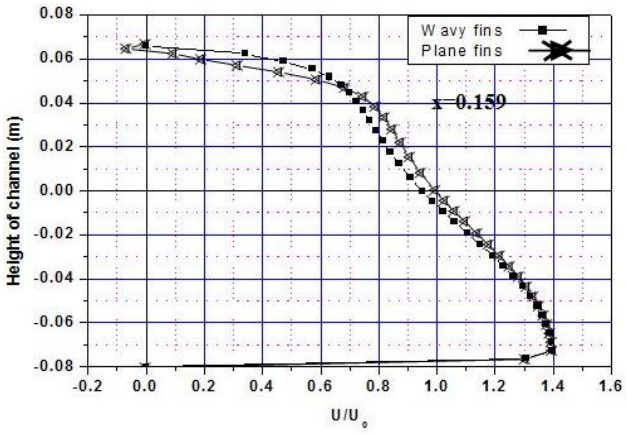

Fig. 2 Comparison of our velocity profile with that of [13] for x = 0.159

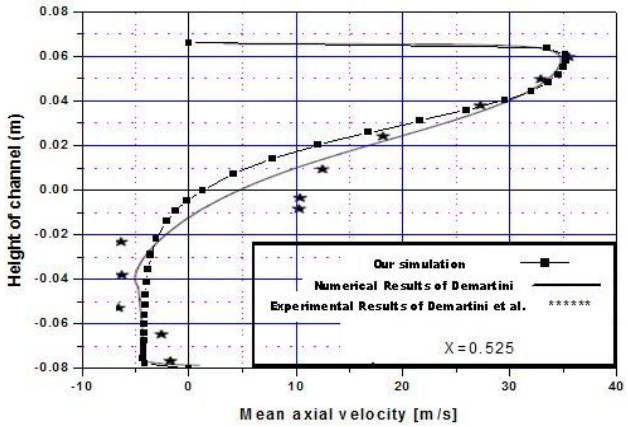

Fig. 3 Comparison of our velocity profile with that of [13] for x = 0.525 m

In the followings we have limited our analysis to study the influence of the waved fins spacing on the dynamic and thermal system.

4.3. Influence of the positions of the fins on the dynamic behaviour

For a Reynolds number equal to 20000, we present the velocity fields respectively for three positions of the two chicanes, corresponding to spacing's equal to s_1 = 0.142 m, Fig. 4, a, $s_2 = s_1/2$ = 0.071 m, Fig. 4, b and $s_3 = 3s_1/2$ = 0.213 m, Fig. 4, c.

These results reveal the existence of three zones (Fig. 4). In the first zone, located just upstream of the block, the fluid flow, comes with a constant velocity *U*. As we approach the first fin, the current lines are deflected and the velocity profiles are more affected by it. The second area is located above the first fin; the air is accelerated by the effect of reducing the flow area. The velocity profiles are almost identical in this area. Finally, the third zone located downstream of the second obstacle is caused by the effect of the expansion of the air leaving the section formed by the fin and the top plate. It can be observed the formation of a recirculating flow whose extent is proportional to the Reynolds number. This phenomenon is illustrated by the negative values profile velocity in this area.

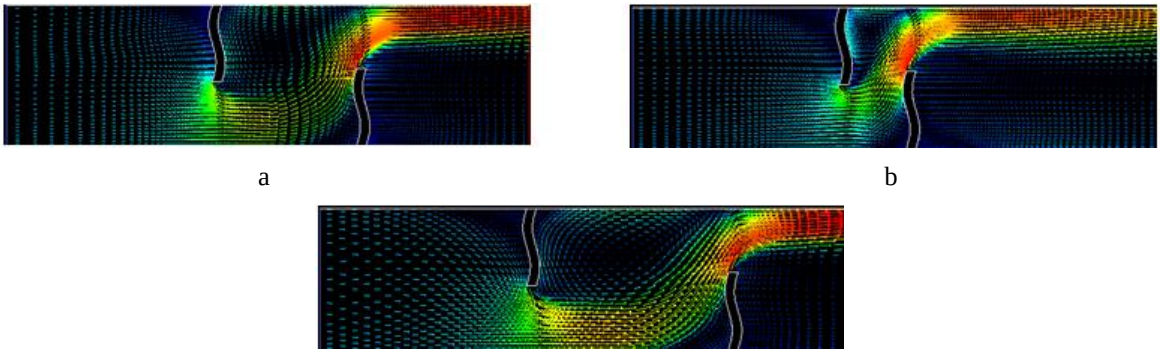

Fig. 4 Velocity field for different spacings of the fins: a) s_1 = 0.142 m, b) s_2 = 0.071 m, c) s_3 = 0.213 m

These results reveal the existence of three zones (Fig. 4). In the first zone, located just upstream of the block, the fluid flow, comes with a constant velocity *U*. As we approach the first fin, the current lines are deflected and the velocity profiles are more affected by it. The second area is located above the first fin; the air is accelerated by the effect of reducing the flow area. The velocity profiles are almost identical in this area. Finally, the third zone located downstream of the second obstacle is caused by the effect of the expansion of the air leaving the section formed by the fin and the top plate. It can be observed the formation of a recirculating flow whose extent is proportional to the Reynolds number. This phenomenon is illustrated by the negative values profile velocity in this area.

The presence of fins creates a vortex and changes not only the flow fields near her, but also the size of the primary vortex. This is because the fin is blocking the movement of fluids and weakens the primary vortex. This dependence shows a distance between fins shorter (case b) brings more changes on the vortex a longer distance (case c), ie, disruption of the flow is inversely proportional to the distance between fins.

4.4. Influence of fin spacing on the thermal comportment

The plot shows that the fluid temperature (Fig. 5) in the vortex region is significantly high as compared to that in the same region of no fins region. In the region downstream of the two corrugated fins, recirculation cells with low temperature are observed. In the regions between the tip of the fins and the channel wall, the temperature is increased. Due to the changes in the flow direction produced by the fins, the highest temperature value appears behind the lower channel wall with an acceleration process that starts just after the first and the second fins.

These results show that the left side of the face corrugated is always better than the cold front that seems right is evident from the moment that the first is the direct target of fresh air. The range of Reynolds number is in line with the increasing number of local Nusselt except on the face corrugated right where there is recirculation of the fluid. These results seem consistent with those obtained experimentally by L.C. Demartini et al, [12].

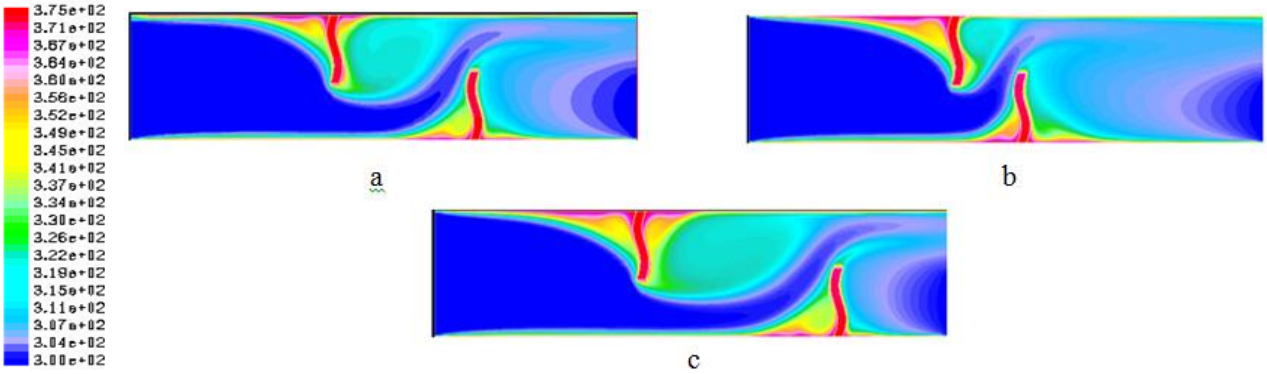

Fig. 5 Temperature field for different spacings between the fins: a) s_1 = 0.142 m, b) s_2 = 0.071 m, c) s_3 = 0.213 m

For the followings, we present the rate of heat transfer characterized by the profile of the Nusselt number determined for the three cases of inter distances fins and four values of Reynolds number: 5000, 10000, 15000 and 20000 respectively in Fig. 6, a-d. The comparison between these four plots shows that the Nusselt number increases with Reynolds number. These profiles present in all cases a minimum and a maximum Nusselt number. The minimum

value is located in the first part of the canal is due at the beginning of warm air in the presence of the first vane located in the upper half of the channel and induces a sharp decrease in speed. The growth of the Nusselt number to its maximum value in the first located in the central part, between the fins and out of the canal is the result of an intense acceleration of the recirculating flow in this area that promotes an increase in heat exchange.

If we think in terms of exchange medium, there is increasing almost linearly Nusselt number as a function of Reynolds number and it is increasingly high as and as one decreases the distance between fins (Fig. 7).

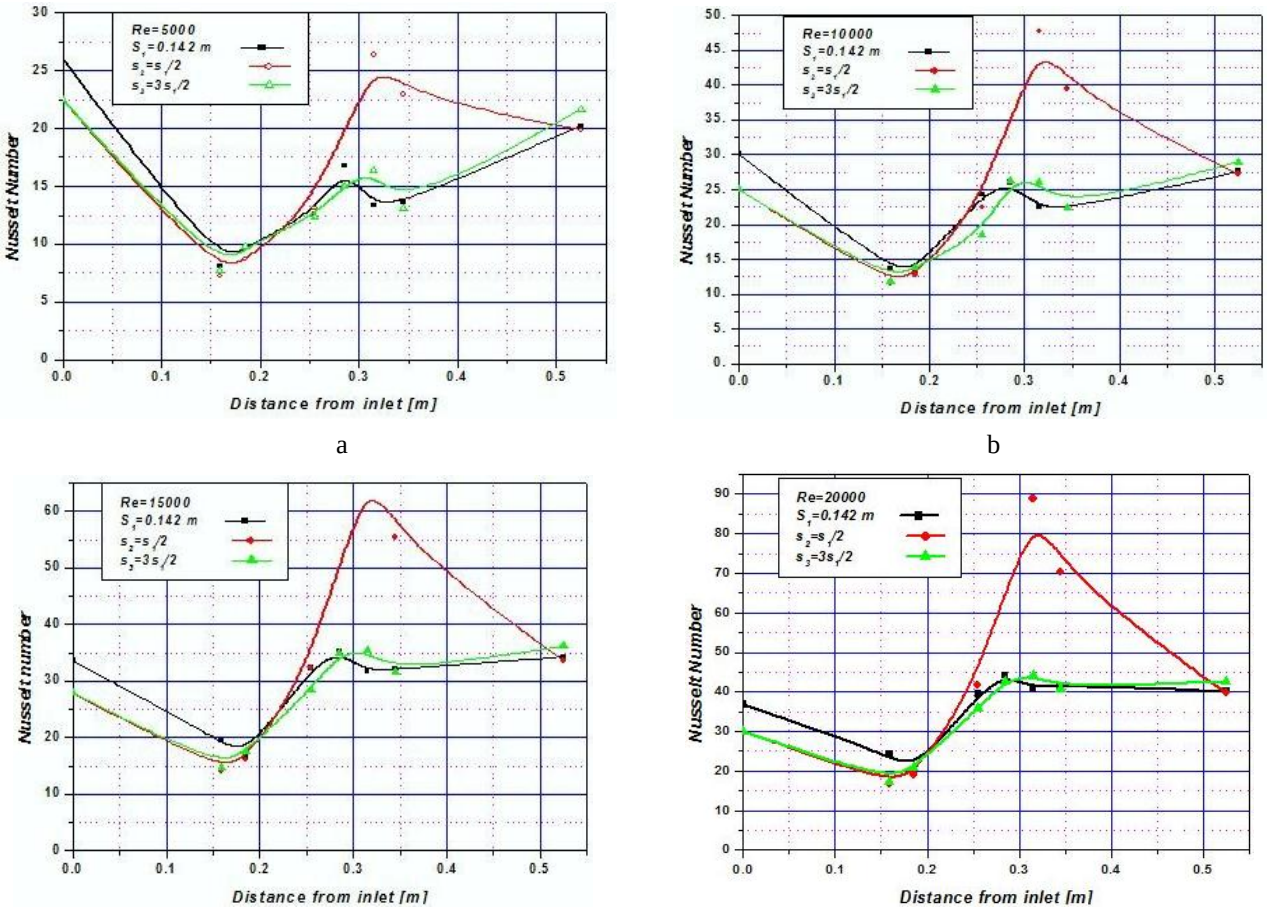

Fig. 6 Nusselt number based on the length of the pipe for three distances cross fins s_1 = 0.142 m, s_2 = 0.071 m, s_3 = 0.213 m; a) Re = 5000, b) Re = 10000, c) Re = 15000, d) Re = 20000

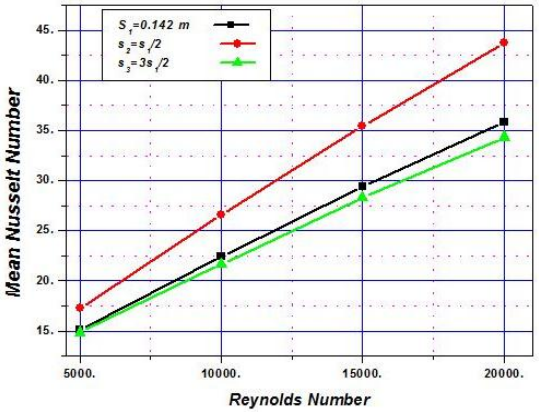

Fig. 7 Number of average Nusselt number as a function of Reynolds varying distances cross fins

From the results in Fig. 7, correlations can be proposed between the average Nusselt number and Reynolds number in the range of Reynolds numbers tested.

- ✓ For s_1 = 0.142 m, $Nu = 4.884\ Re^{0.6241}$
- ✓ For $s_2 = s_1/2$ = 0.071 m, $Nu = 17.064\ Re^{0.6695}$
- ✓ For $s_3 = 3s_1/2$ = 0.213 m, $Nu = 14.627\ Re^{0.6045}$

4.5. Effect of the location of the fins on the coefficient of friction

Fig. 8, a-d show the profiles of the coefficients of friction for the four Reynolds numbers tested. It is found that the friction is almost negligible at the beginning of the area upstream of the first waved fins, and it grows increasingly approaching the first fin and especially in the area between the two fins. These figures also present that reducing the distance between fins increases the friction coefficient that reflects the intensity of fluid motion in this area. We see this clearly in the case of $s_2 = s_1/2$ example, or the maximum values of the coefficient of friction is between the fins, because the direction of flow of primary turns dramatically causing friction intermolecular charge-air and between air and walls on the other.

Similarly, from these curves, we can see that the coefficient of friction increases with decreasing distance between the fins and increasing the Reynolds number, (Fig. 9). Correlations based on it can be proposed.

- ✓ For s_1 = 0.142 m, $C_f = 0.0005\ Re^{1.6333}$
- ✓ For $s_2 = s_1/2$ = 0.071 m, $C_f = 0.0008\ Re^{1.7464}$
- ✓ For $s_3 = 3s_1/2$ = 0.213 m, $C_f = 0.0006\ Re^{1.6306}$

We find the same remarks mentioned above ie a growth of pressure losses depending on the Reynolds number with maximum values corresponding to short distances cross fins. It also increases slightly to a Reynolds number below to 15000 by the undulation of the fin allows the fluid to move with light friction, but after this value we find that it increases sharply as a function of Reynolds number increases. Thus the use of auxiliary surfaces of vane type is useful for improving heat transfer in pipes and upgrading of interchanges in general, but nevertheless has a major drawback of the pressure losses that are potentially high. This observation is confirmed by the work of research Gruss [16, 17] and Thonon et al [18].

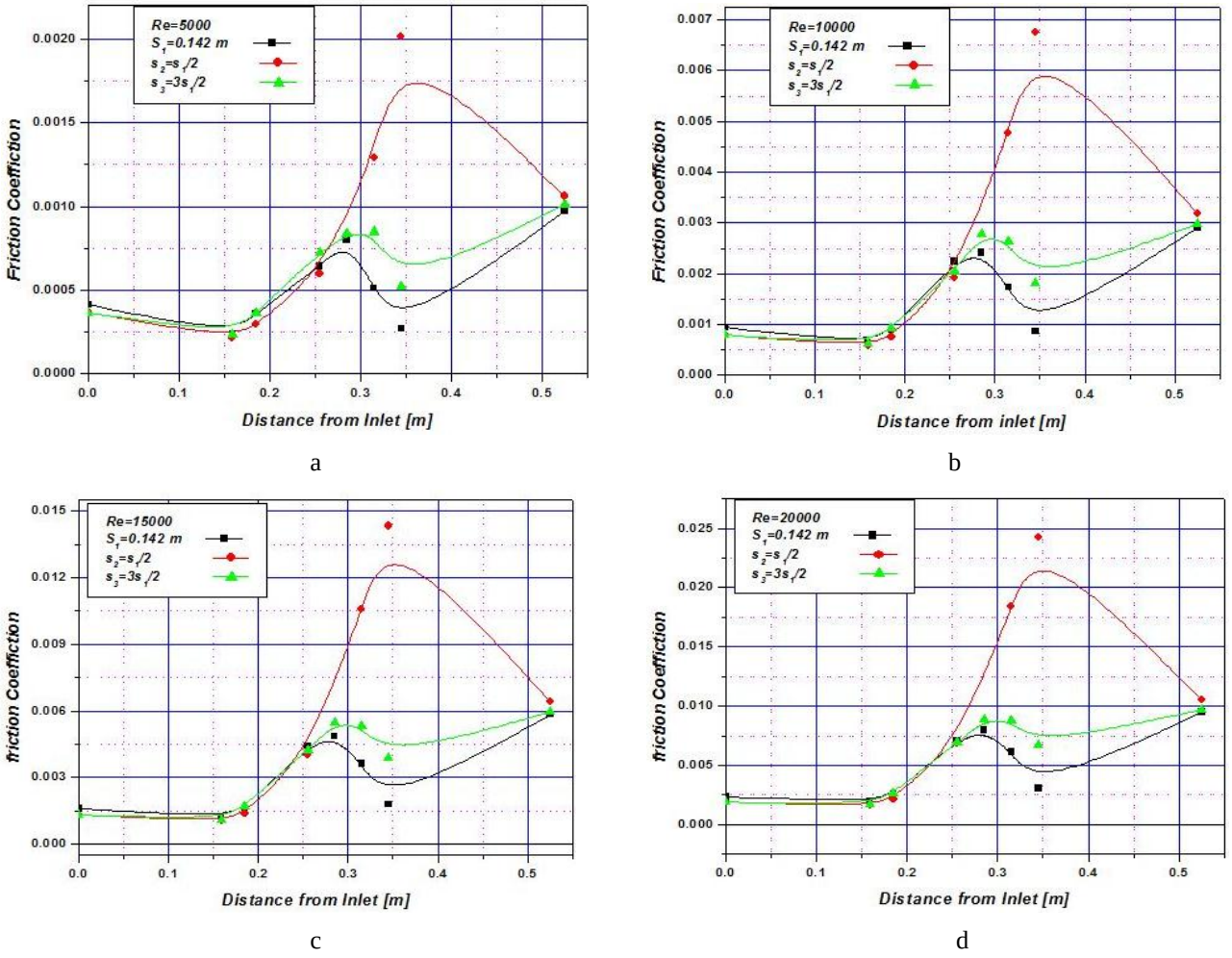

Fig. 8 Distribution of coefficients of friction for the three distances cross vanes: a) *Re* = 5000, b) *Re* = 10000, c) *Re* = 15000, d) *Re* = 20000

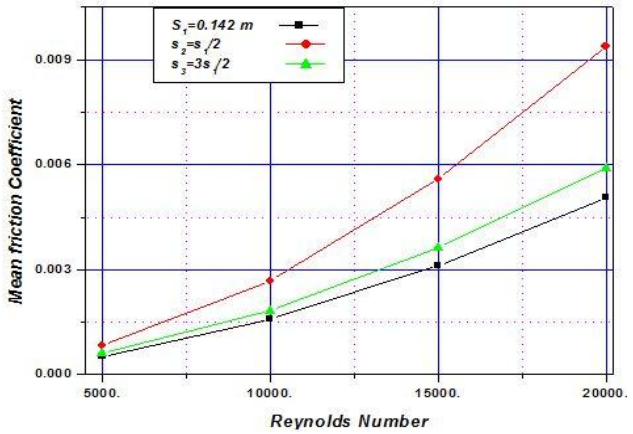

Fig. 9 Variation of average friction coefficient as a function of Reynolds number varying distances cross fins

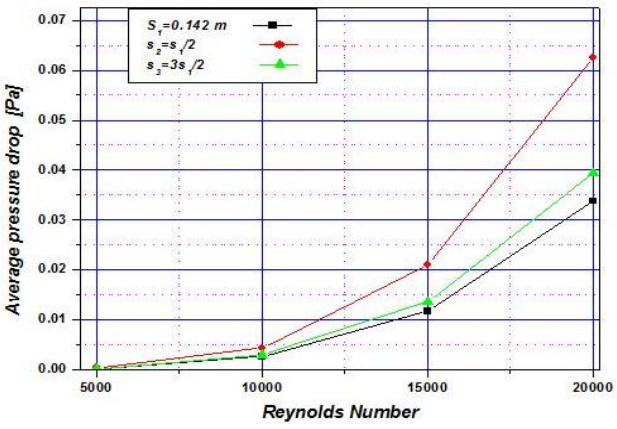

Fig. 10 Pressure drop as a function of Reynolds number varying distances cross fins

5. Conclusion

A numerical study of heat transfer by turbulent forced convection is proposed in a rectangular channel with two corrugated fins in order to increase the phenomena of friction and heat transfer. The effects of positions and distances of inter waved fins on dynamic comportment and heat flow was examined for four Reynolds numbers. The results show that decreasing the distance between the fins causes a substantial increase in the Nusselt number and pressure loss. Increasing the Reynolds number increases the heat transfer but removes the ripple effect of fins on the pressure reduction after a value equal to 15000. The use of corrugated fins in heat exchangers is effective in such systems could lead to lower consumption of energy resource, which provides benefits to both economic and environmental aspects.

References

1. **Nasiruddin, M.H.; Kamran., S.** 2007. Heat transfer augmentation in a heat exchanger tube using a baffle, International Journal of Heat and Fluid Flow 28(2): 318-328. http://dx.doi.org/10.1016/j.ijheatfluidflow.2006.03.020.
2. **Fiebig, M.; Kallweit, P.; Mitra, N.; Tiggel, B.S.** 1991. Heat transfer enhancement and drag by longitudinal vortex generators in channel flow, J. Exp. Thermal Fluid Sci 4: 103-114. http://dx.doi.org/10.1016/0894-1777(91)90024-L.
3. **O'Brien, J.E.; Sohal, M.S.; Wallstedt, P.C.** 2004. Local heat transfer and pressure drop for finned-tub heat exchanger using oval tubes and vortex generators, J. Heat Transfer 126: 826-835. http://dx.doi.org/10.1115/1.1795239.
4. **Roetzel, W.; Lee, D.W.** 1994. Effect of baffle/shell leakage flow on heat transfer in shell-and-tube heat exchanger, Experimental Thermal and Fluid Science 8: 10-20. http://dx.doi.org/10.1016/0894-1777(94)90068-X.
5. **Rajendra, K.; Maheshwarib, B.K.; Karwac, N.** 2005. Experimental study of heat transfer enhancement in an asymmetrically heated rectangular duct with perforated baffles, International Communications in Heat and Mass Transfer 32: 275-284. http://dx.doi.org/10.1016/j.icheatmasstransfer.2004.10.002.
6. **Gupta, B.B.; Howell, J.A.; Wu, D.; Field, R.W.** 1995. A helical baffle for cross-flow microfiltration, Journal of Menbrane Science 99: 31-42. http://dx.doi.org/10.1016/0376-7388(94)00241-P.
7. **Yong-Gang Lei; Ya-Ling He; Pan Chu; Rui Li** 2008. Design and optimization of heat exchangers with helical baffles, Chemical Engineering Science 63: 4386-4395 G. http://dx.doi.org/10.1016/j.ces.2008.05.044.
8. **Kang-Hoon Ko; Anand, N.K.** 2003. Use of porous baffles to enhance heat transfer in a rectangular channel, International Journal of Heat and Mass Transfer 46: 4191-4199. http://dx.doi.org/10.1016/S0017-9310(03)00251-5.
9. **Ahmet Tandiroglu** 2006. Effect of flow geometry parameters on transient heat transfer for turbulent flow in a circular tube with baffle inserts, International Journal of Heat and Mass Transfer 49: 1559-1567. http://dx.doi.org/10.1016/j.ijheatmasstransfer.2006.01.018.
10. **Molki, M.; Mostoufizadeh, A.R.** 1989. Turbulent heat transfer in rectangular ducts with repeated-baffle blockages, Int. J. Heat Mass Transfer. 32(8): 1491-1499. http://dx.doi.org/10.1016/0017-9310(89)90071-9.
11. **Rajendra Karwa; Maheshwari, B.K.** 2009. Heat transfer and friction in an asymmetrically heated rectangular duct with half and fully perforated baffles at different pitches, International Communications in Heat and Mass Transfer 32: 264-268. http://dx.doi.org/10.1016/j.icheatmasstransfer.2008.11.005.
12. **Hinze, J.O.** 1975. Turbulence, McGraw-Hill, 790 p.
13. **Demartini, L.C.; Vielmo, H.A.; Möller, S.V.** 2004. Numeric and Experimental Analysis of the Turbulent Flow through a Channel With Baffle Plates, J. of the Braz. Soc. of Mech. Sci. & Eng 26(2) 153-159. http://dx.doi.org/10.1590/S1678-58782004000200006.
14. **Patankar, S.V.** 1980. Numerical Heat Transfer and Fluid Flow, Hemisphere/McGraw-Hill, New York.
15. **Endres, L.A.M.; Moller, S.V.** 2001. On the fluctuating wall pressure field in tube banks, Nuclear Engineering and Design 203: 13-26. http://dx.doi.org/10.1016/S0029-5493(00)00293-4.
16. **Gruss, J.A.** 2002. Les micro échangeurs thermiques, Techniques de l'Ingénieur- Rubrique Innovations, Référence IN3.
17. **Gruss, J.A.** 2004. Etat de l'art sur les échangeurs à microstructures, Rapport technique confidentiel, GREThh, CEA/DTEN/DR/2004/024.
18. **Thonon, B; Marty, P.** 2003. Micro thermal systems in France: From knowledge to technological development, Conference Microchannels and Minichannels – Rochester, 15-23.

H. Benzenine, R. Saim, S. Abboudi, O. Imine

PRIVERSTINIO-KONVEKCINIO TURBULENTINIO ŠILUMOS SRAUTO PERDAVIMO ORUI KANALE SU BANGUOTŲ BRIAUNŲ GRIOVELIAIS SKAITINĖ ANALIZĖ

R e z i u m ė

Šiame darbe pateikti srauto struktūros ir konvekcinio šilumos perdavimo plokščiame kanale su banguotų briaunų grioveliais viršutinėje ir apatinėje stačiakampio skerspjūvio kanalo sienelėse skaitinio tyrimo rezultatai. Šiuose tyrimuose skirtingų Reinoldso skaičių (5000, 10000, 15000 ir 20000) kanalai atitinka nusistovėjusį turbulentinį srautą. Vyraujančios lygtys (tolydumo, momentų, energijos ir turbulentiškumo) išspręstos naudojant atitinkamas kietojo kūno ir skysčio zonų savybes. Kontrolinio tūrio priartėjimas panaudotas diskretizuojant būvio lygtis skaitiniam sprendimui. Modelis *k-ω* pritaikytas turbulentinio srauto laukui. Paprastas algoritmas panaudotas konvekcijai įvertinti. Kompiuterinė programa pritaikyta dinaminei ir terminei elgsenai įvertinti esant keturioms Reinoldso skaičių reikšmėms ir skirtingoms geometrinėms briaunų padėtims. Ašinio greičio profiliai įvertinti konvek-

ciniu Nuselto skaičiumi, trinties koeficientai ir slėgio kritimai skirtinguose pasirinktuose skerspjūviuose rasti kaip tik prieš srovę, pagal srovę ir tarp dviejų banguotų briaunų.

H. Benzenine, R. Saim, S. Abboudi, O. Imine

NUMERICAL STUDY ON TURBULENT FLOW FORCED-CONVECTION HEAT TRANSFER FOR AIR IN A CHANNEL WITH WAVED FINS

S u m m a r y

This paper presents a numerical study on flow structure and convective heat transfer in a plane channel with waved fins mounted alternatively on top and bottom of the walls in a rectangular channel. In this investigation or different bar sizes in the Reynolds number range (5000, 10000, 15000 and 20000) corresponding to steady turbulent flow. The governing equations (continuity, momentum, energy and the turbulence) are solved over the entire domain, using the corresponding properties for the solid and fluid regions. The control volume approach is employed in order to discredit the governing equations for their numerical solution. The *k*-*ω* model has been applied to the turbulent flow field. The SIMPLE algorithm was used for the convective terms in the solution equations. A computer code was developed to study the dynamic and thermal comportment for four values of Reynolds number and for different geometric positions of the fins. The axial velocity profiles, the structures represented by the convective Nusselt number, the coefficients of friction and pressure losses were obtained for various selected sections, namely, upstream, downstream and between the two waved fins.

Keywords: Forced convection, turbulent flow, waved fins, finite volume, numerical analysis.

Received November 23, 2011
Accepted March 04, 2013